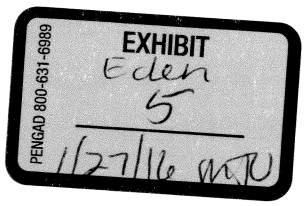

December 2003
Volume 42 Number 12
ISSN 0091-3286

OPTICAL ENGINEERING

SPIE—
The International
Society for
Optical Engineering

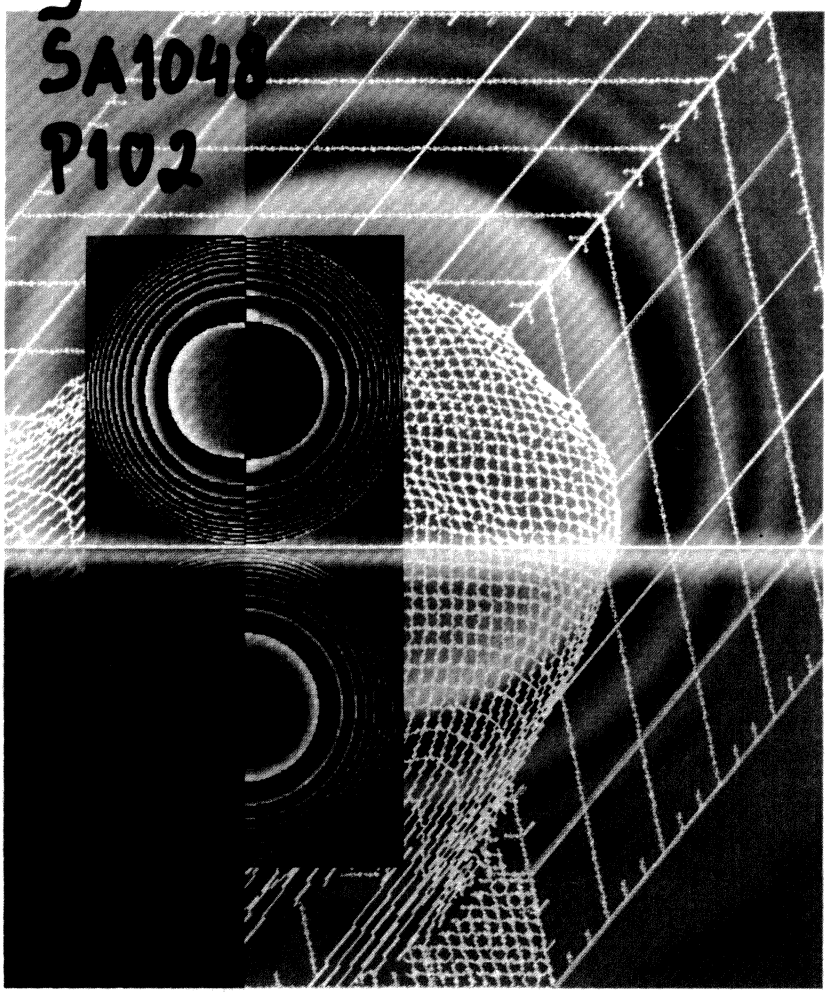

- OE Letters

Acousto-Optical Tunable Filters
Diffractive Optics
Optical Clock Generation
Optical Logic Generation
Optical Switches
Waveguide Gratings
Wavelength Monitors

- Featuring Papers on

Automated Visual Inspection
Crack Measurement
Digital Holography
Fiber Amplifiers
Fiber Bragg Gratings
Fiber Dispersion
Image Reconstruction
Image Restoration
Infrared Beamsplitters
Infrared Detectors
Infrared-to-Visible Converters
Interferometry
Laser Heat Treating
Liquid Crystals on Silicon
Motion Blur
Optical Encryption
Optical Sensors
PLZT Thin Films
Polarizers
Position Estimation
Profilometry
Radiometric Calibration
Time-of-Flight Range Finders
Ultraviolet Lasers
X-Ray Optics

This resource is also available
on the WWW.
Use MadCat to launch.

OPTICAL ENGINEERING

Donald C. O'Shea
Editor

Mailing:
SPIE
P.O. Box 10
Bellingham, Washington 98227-0010

Shipping:
SPIE
1000 20th Street
Bellingham, Washington 98225
360/676-3290 • Fax 360/647-1445
E-mail journals@spie.org

Editorial. Send manuscripts and technical correspondence to SPIE. Papers and reviews published in *Optical Engineering* reflect the opinion of the author(s); inclusion of articles and advertisements does not necessarily constitute endorsement by the editors or by SPIE.

SPIE Membership. Annual membership dues include a choice of the Society's four peer-reviewed journals. 2003 membership dues: $95; $45 Retired; $40 Student. For more information, contact SPIE Membership Services at 360/676-3290, Fax 360/647-1445, e-mail: membership@spie.org. **Change of Address.** Send old and new address to SPIE Headquarters.

Optical Engineering (ISSN 0091-3286) (USPS 450-970) is published monthly by the Society of Photo-Optical Instrumentation Engineers, 1000 20th St., Bellingham, WA 98225 at the following annual subscription prices: print plus online, $550 N. America, $615 outside N. America. Periodicals postage paid at Bellingham, WA 98225, and at additional mailing offices. **Postmaster:** Send address changes to *Optical Engineering*, 1000 20th St., Bellingham, WA 98225.

Printed in the United States on acid-free paper.

Contributions for optics education. SPIE, a nonprofit public benefit corporation, gratefully accepts tax-deductible contributions and bequests in support of its efforts to foster interaction and to advance knowledge in optical and optoelectronic applied science and engineering. With special emphasis on education, SPIE annually awards scholarships and publishes a guide to optics programs in colleges and universities around the world. The Society has established a fund to support student travel to SPIE symposia and is facilitating donations of technical publications to educational institutions and libraries without access to this literature. For information on how you can contribute or participate in a deferred-giving program, please contact Sharon Kirkpatrick, SPIE Headquarters, P.O. Box 10, Bellingham, WA 98227-0010, 360/676-3290, Fax 360/647-1445, E-mail sharonk@spie.org.

Optical pumping of the XeF(C→A) and iodine 1.315-μm lasers by a compact surface discharge system

B. A. Knecht*
R. D. Fraser†
D. J. Wheeler‡
C. J. Zietkiewicz§
A. A. Senin, MEMBER SPIE
L. D. Mikheev‖
V. S. Zuev‖
J. G. Eden
University of Illinois
Department of Electrical and Computer Engineering
Laboratory for Optical Physics and Engineering
Urbana, Illinois 61801

Abstract. Details are provided regarding the design, construction, and performance of a compact (≈0.6-m^2 footprint), single-channel surface discharge system and its application to optically pumping the XeF(C→A) and iodine atomic lasers in the blue-green (≈480 nm) and near infrared (1.315 μm), respectively. The system has a gain (active) length of ≈50 cm, and triggering the discharge requires no high-voltage or high-current switches. Measurements of the velocity of the photodissociation bleaching wave and the small-signal gain of the XeF(C→A) system are described. At 488 nm, the gain coefficient γ was found to be ≈0.3% cm^{-1}, a value comparable to those reported previously for systems dissipating considerably higher power per unit length. Single-pulse energies >50 mJ from the XeF(C→A) laser (≈485 nm) and >0.7 J on the $5p\,^2P_{1/2}\rightarrow 5p\,^2P_{3/2}$ transition of atomic iodine at 1.315 μm have been obtained with nonoptimized resonator output couplings (5% and 10%, respectively). The rate of erosion of the dielectric surface has been measured to be ≈0.1 to 0.3 μm/shot for a glass ceramic dielectric, and the performance of two electrical configurations for the ballasting pins (feedthrough and V) is compared. [DOI: 10.1117/1.1624849]

Subject terms: lasers; visible; optical pumping; surface discharge.

Paper 030139 received Mar. 24, 2003; revised manuscript received Jun. 9, 2003; accepted for publication Jun. 10, 2003.

1 Introduction

The surface discharge, an electric discharge at the interface of a gas and a solid dielectric, was first reported by G. C. Lichtenberg in 1777. Over the past three decades, renewed interest in surface discharges has been driven by potential applications in materials processing,[1] surface cleaning,[2,3] waste remediation, and optical pumping of lasers by photodissociation,[4–6] all of which require intense sources of ultraviolet (UV) or vacuum ultraviolet (VUV) radiation.

Excitation of lasers by a surface discharge is particularly attractive because of the ability of the optical source to produce quasi-blackbody radiation having a characteristic temperature above 3×10^4 K and to do so with a relatively simple system amenable to repetitively pulsed operation. In 1975, Beverly[5] proposed pumping the iodine photodissociation laser ($5p\,^2P_{1/2}\rightarrow 5p\,^2P_{3/2}$; $\lambda = 1.315$ μm) with a surface discharge and subsequently measured efficiencies approaching 10% and 3% for the conversion of electrical power to optical radiation in the 250- to 290-nm and 170- to 210-nm spectral regions, respectively.[7] Studies have also shown surface discharges to be effective sources of extreme ultraviolet (XUV; $\hbar\omega\approx 10$ to 70 eV) photons,[3] and characteristic radiation temperatures of $(1\text{ to }2)\times10^4$ K are attainable for specific energy loadings of the plasma of 1 to 4 J cm^{-2} (Ref. 5). In 1979, Belotserkovets et al.[8] demonstrated lasing from atomic iodine when the molecular precursor, C_3F_7I, was photolyzed by a surface discharge. Since that time, a variety of atomic and molecular lasers initiated or pumped entirely by a surface discharge have been demonstrated,[4,9] but much of the effort has been directed toward the XeF photodissociation laser,[10,11] partly because of the breadth of the absorption spectrum of the parent molecule, XeF_2. The other factors providing impetus for the efforts on XeF are the two laser transitions that are available (B→X and C→A) as well as the large saturation intensity of the C→A band in particular.[12] The latter, ≈400 kW cm^{-2}, is a direct reflection of both the C-A stimulated emission cross section ($\approx 9\times10^{-18}$ cm^2) and the C-state radiative lifetime (93±5 ns).[13]

In a series of papers published between 1984 and the early 1990s (Refs. 14 to 17), Kashnikov, Zuev and coworkers reported the characteristics of a sequence of surface-discharge-pumped XeF laser systems producing as much as 174 J on the B→X transition of the molecule in

*Present address: 662N 300W, Lebanon, IN 46052.
†Present address: Realized Technologies Inc., 1530 Barclay Blvd., Buffalo Grove, IL 60089.
‡Present address: National Center for Supercomputing Applications (NCSA), University of Illinois, 605 E. Springfield, Champaign, IL 61820.
§Present address: Melles Griot, 2605 Trade Center Avenue, Longmont, CO 80503.
‖Permanent address: P. N. Lebedev Physical Institute, Moscow, Russian Federation.

the UV at 351 nm and up to 117 J in the blue-green (C $\rightarrow$A transition, $\lambda \approx 485$ nm). Consisting of individual discharge sections, each typically 8 to 12 cm in length and having a dedicated capacitor and high-voltage switch, these optical sources had active lengths ranging from 70 to 190 cm. The first system, reported by Kashnikov et al.,[14] comprised eight discharge sections in a single-channel design and yielded a brightness temperature of $\approx 3 \times 10^4$ K. By increasing the gain length to 190 cm (16 discharge sections), raising the number of discharge channels to three, and with careful attention given to the current rise time and the purity of the XeF_2 vapor, the Russian group subsequently produced single-pulse energies that are, to this day, unsurpassed for a primary coherent source in the visible.[17]

Despite the impressive characteristics of these lasers, including the ability to operate at a pulse repetition frequency of 1 Hz, the system was quite large, and the dedication of a capacitor and high current switch to each discharge section introduced significant timing jitter (<0.25 μs). Furthermore, in low-impedance circuits of this type, switches consume substantial energies and adversely affect the complexity and lifetime of the system.

In the mid-1990s, we reported the design and preliminary operation of a compact surface discharge system that successfully pumped the XeF(C$\rightarrow$A) and iodine photodissociation lasers.[18,19] A more detailed account of the design and operation of this system and an alternative structure for the surface discharge ignition electrodes are presented here. Having an active length of ≈ 50 cm, this surface discharge system requires no high-voltage (or high-current) switches, which has the beneficial result of lowering the firing jitter as well as the equivalent series inductance for the system. Careful attention given to the design and layout of the device and the power generator has resulted in a rugged system having a compact footprint (≈ 0.6 m^2) and an overall size comparable to that of a commercial excimer laser. The small-signal gain on the C$\rightarrow$A transition of XeF has been measured to be 0.3% cm^{-1} at 488 nm, a value virtually identical to those reported for surface discharge systems of considerably higher power loadings.

This paper is organized as follows. Section 2 describes in detail the design of the electrical system and laser head for the device. Two approaches to igniting the surface discharge, surface feedthrough (in-line) and V configurations, are presented and compared. The experimental results on the XeF(C$\rightarrow$A), XeF(B$\rightarrow$X), and atomic iodine (1.315 μm) lasers are discussed in Sec. 3, and Sec. 4 summarizes the conclusions of this study.

2 Surface Discharge System: Design and Performance

2.1 *Background*

Previous designs of surface discharge systems can be broadly classified into two groups. The first are those in which the discharge occurs on a dielectric surface such as polyethylene, Teflon, or a ceramic[9,14–17] and the distance d between consecutive electrodes ranges from several centimeters to beyond 10 cm. The practical upper limit on the discharge gap is dictated by the breakdown voltage for a given surface and the spatial instability of the discharge,

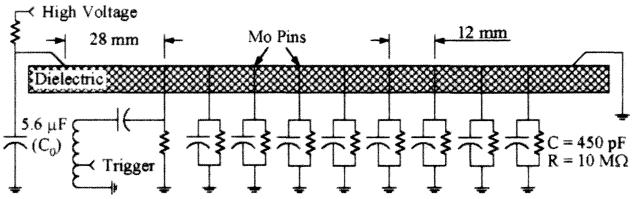

Fig. 1 Schematic diagram of the feedthrough (in-line) electrical configuration for igniting and sustaining a surface discharge. The Mo pins are ballasted capacitively and resistively, and the charging voltage is typically 30 kV. The dielectric surfaces explored to date are machinable glass ceramic, BN, and Al_2O_3 and SiC-coated surfaces.

which rises dramatically with increasing d. If no accommodations are made for triggering the discharge or preionizing the gap, charging voltages of $\gtrsim 15$–30 kV are required, even for small gaps ($d \approx 2$–3 cm), to obtain an adequate radiation temperature. Systems with long gain lengths, such as the devices of Refs. 14–17, having active lengths of 0.7–1.9 m, rely on discharge sections operated in tandem. Each section, typically 8–12 cm in length, requires 10 kV when the entire discharge is triggered by a 50-kV pulse applied to a cable lying beneath the dielectric surface. The device of Ref. 16, for example, had a gain length of 1.9 m as a result of 16 individual discharge sections, each 12 cm in length.

The second general category of devices relies on discharges produced on the surface of ferrite rods or slabs. Producing a stable, intense surface discharge with these materials requires forming a channel in the ferrite, either by exploding a wire on its surface[20] or by micromachining a narrow channel (≈ 150 μm) by laser ablation.[21] Such devices typically involve rods tens of centimeters in length (76 cm in Ref. 20) and driven by a capacitor charged to 40 to 50 kV. To summarize, realizing in a surface discharge system the gain lengths normally required for high-power laser operation (tens of centimeters) requires a means for spatially confining the discharge. Long path lengths can be obtained with ferrites once a channel has been established on the surface, or shorter discharge sections (≈ 10 cm) can be combined in tandem to yield active lengths beyond 1 m.[20–24]

2.2 *Electrical Design: Power Generator and Discharge Ignition Configurations*

The approach adopted for the experiments reported here offers a novel and robust scheme for establishing surface discharges over paths of arbitrary length and to do so without the need to switch each section independently. In fact, no high-current or high-voltage switches are used at all. Rather, the discharge functions as its own switch.

A schematic diagram of the first electrode configuration investigated is shown in Fig. 1. The key elements of this surface discharge device are: a ceramic substrate that runs parallel to the discharge axis, a main electrode at each end, and a series of intermediate electrodes between the main electrodes which divide the discharge path into segments. The critical feature of this design is the latter—a series of resistively and capacitively-ballasted molybdenum pins, which serve to both establish and stabilize the surface dis-

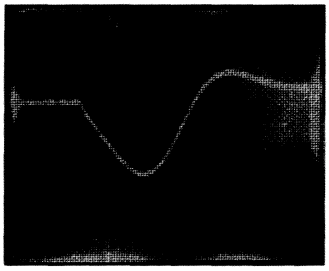

Fig. 2 Oscillogram of the surface discharge current for a charging voltage of ≈30 kV. The horizontal (temporal) scale is 2 μs/div, and the vertical scale is 20 kA/div.

charge. All of the pins in the linear array were isolated from dc ground by a 10-MΩ resistor and a 450-pF doorknob capacitor. For the first pin (trigger electrode), however, the capacitor was connected in series with the secondary of an air-core autotransformer, to which the trigger pulse was applied. The separation between the pins in the array, except that between the high-voltage (HV) and trigger electrodes was set at 12.7 mm (1/2 in.) to ensure that breakdown between two adjacent pins occurred at or below 30 kV when the gas pressure in the laser chamber was 1 atm. The gap between the HV electrode (left side, Fig. 1) and the trigger electrode was set to 28 mm (designed to hold off 30 kV). Consequently, when the full supply voltage was impressed across the entire array (HV electrode to ground), breakdown does not occur in the absence of a trigger pulse. However, when a −15 to −18-kV trigger pulse is applied to the transformer primary, the voltage appearing on the first pin (trigger electrode) is −50 kV, and breakdown occurs in the HV-electrode–trigger-electrode gap. As current begins to flow in this gap, the voltage at the trigger electrode rises rapidly to a value slightly *above* 30 kV, owing to peaking effects. Since the second pin in the array is still at ground potential, the gap between the trigger electrode (pin 1) and pin 2 now self-breaks. The remaining gaps in the array follow in quick succession, and within 5 μs of the application of the trigger pulse, a surface discharge is established along the entire length of the array. A major advantage of this design is that the individual gaps are not triggered independently and, consequently, the firing jitter (with respect to the command trigger) is low. Furthermore, although negative trigger pulses were normally employed in the experiments described here, the use of an autotransformer reduces the sensitivity of the system to the polarity of the trigger (because of ringing in the secondary of the transformer), resulting in improved reliability and stability.

Little of the energy stored in the capacitor bank (5.6 μF cf. Fig. 1) is expended in forming the discharge, but the establishment of the surface discharge presents a low-impedance path to ground. It is at this point that C_0 delivers virtually all of its stored energy to the discharge, resulting in rapid heating of the plasma and the generation of intense blackbody radiation. It should be mentioned that once the discharge is established, negligible current flows through the ballasting pins, which are effectively decoupled from ground.

Figure 2 is an oscillogram of the discharge current, obtained with 1 atm of air in the laser head and a machinable glass ceramic (MACOR) serving as the dielectric. The

Fig. 3 Photograph of the surface discharge. The path length is 48.5 cm.

waveform, recorded by a modified Rogowski coil for a charging voltage on the capacitor bank of 30 kV, is representative of those observed throughout these experiments and shows that the current reaches its peak value of ≈46 kA in ≈4 μs. The maximum current observed to date is >50 kA. Notice that the current waveform is essentially critically damped, indicating that the impedance of the capacitor bank nearly matches that of the surface discharge. This is a result of efforts from the earliest designs to minimize the inductance of the power generator and laser head. Consequently, >80% of the 2.5 kJ stored in the capacitor bank (for $V=30$ kV) is deposited in the surface discharge in the first half cycle of the current waveform. For a power pulse having a temporal width of 5 μs (FWHM), this energy dissipation corresponds to a power deposition per unit length of discharge of ≈8 MW cm^{-1}.

The low overall inductance of the capacitor bank and electrical connections to the HV and ground electrodes manifested itself in an unusual way during the testing of this system. Early versions of the laser employed standard wire to connect the ballast circuitry to the intermediate electrodes. To facilitate the rapid assembly of the laser head, the wire was later replaced by short springs, but experience showed that it was necessary to carefully limit the number of turns in the coils. Otherwise, the inductive voltage drop produced across the spring resulted in arcing and severe damage to the coil and associated components.

Although the primary purpose of the Mo pins is to enable the rapid formation of a surface discharge over a path of arbitrary length with a moderate voltage, the pin array also serves to confine the discharge, thereby improving the shot-to-shot reproducibility with respect to previous surface discharge devices. Figure 3 is a photograph of the surface discharge viewed normal to the surface. Minor deviations from a straight path are evident, and the overall length of the surface discharge is 48.5 cm.

2.3 *Laser Head: In-Line and V Configurations*

Side, frontal, and end-on views of the laser head with the in-line ballast pin array configuration described in the last section are illustrated schematically in Fig. 4. Each Mo pin was inserted into a cylindrical hole in the dielectric material and was mounted so that its tip was flush with the surface of the dielectric. For most of the experiments reported here, MACOR machinable ceramic served as the dielectric material, but preliminary tests with pyrolytic boron nitride, alumina, and SiC-coated surfaces were also conducted. Because of its chemical stability in the presence of fluorine, Kynar® was the material from which the laser head was machined. The lower plate (not shown in Fig. 4) sealing the laser head was fabricated from a polycarbonate or aluminum. As noted earlier, both the main electrodes and the intermediate (pin) electrodes enter the laser head through the top and traverse the ceramic dielectric. The seal around the main electrodes consisted of a Kynar fitting having a

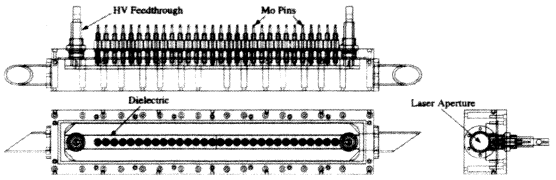

Fig. 4 Drawings (to scale) of the laser head, showing side (top), front (lower left), and end-on views of the Mo pin array, the HV and ground feedthroughs (at the left and right sides of the side and frontal drawings, respectively), and the dielectric itself. For clarity, the lower plate of the laser head has been removed.

tube boss seal on one end and a Swagelok®-compatible seal on the other. Both of the main electrodes themselves were machined from molybdenum (chosen for the purpose of minimizing material ablation per shot) and attached to an aluminum shaft that provided direct electrical contact to the capacitor bank. A detailed diagram of the main electrode feedthrough is provided in Fig. 5. Denoted C_0 in Fig. 1, the capacitor bank comprises 44 low-inductance (equivalent series inductance ≈ 50 nH) capacitors having a rated voltage of 40 kV and connected in parallel. The entire bank is mounted in an Al and polycarbonate enclosure that is quite compact. When fully assembled, the capacitor bank and laser head together have a footprint of only 0.6 m^2 ($150 \times \approx 40$ cm^2), comparable to that for a commercially available excimer laser.

The major drawback of the in-line intermediate electrode design is the failure mode. Particulates formed by the discharge tend to become lodged around the electrodes and gradually migrate into the cylindrical cavities in the ceramic substrate. Consisting of ablated ceramic material and ash produced when the plasma comes in contact with Kynar, the particulates are weakly conductive. The result is an alternate discharge path between the main electrodes and the ground plane on the exterior of the laser head, a path that is no less favorable (from an electrical perspective) than the one intended. The diversion of current into this auxiliary channel produces strong heating of the intermediate electrode insulating sleeve and the surrounding ceramic, often resulting in damage to both the ceramic and the laser head. Periodic cleaning of the laser-head surfaces ameliorates this problem, and installing a closed-loop gas recirculation system to trap particulates should largely eliminate it.

Nevertheless, in an effort to bypass this difficulty through electrode design, a second electrode configuration, known as the V, was designed and demonstrated. End-on and frontal views of the V configuration are illustrated in Fig. 6. One asset of this design is that, by bringing the intermediate electrodes to the dielectric surface at an oblique angle and from alternating sides of the laser chamber, the fabrication and installation complexities associated with introducing electrodes through the dielectric are eliminated, and replacing the dielectric is greatly simplified. Furthermore, the distance between the electrode shanks on a given side of the laser chamber is maximized. Although this approach eliminated the damaging misfires experienced with the in-line configuration, particulates deposited on the laser chamber wall caused occasional flashover between the intermediate electrodes. Our experience is that this drawback can be rectified by periodic cleaning and, presumably, a particulate trapping system.

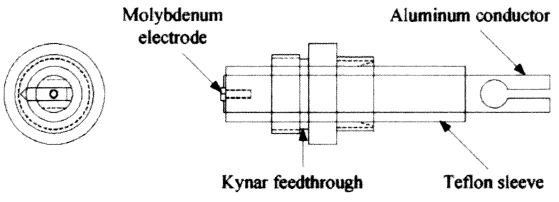

Fig. 5 Diagram (to scale) of the main electrode feedthrough, showing end-on (left) and side views of the assembly.

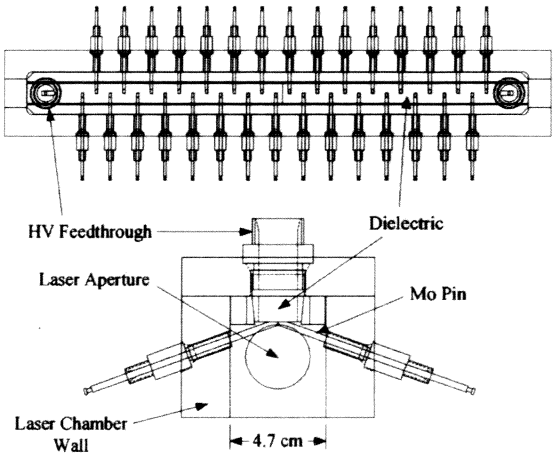

Fig. 6 Front (upper panel) and end-on (lower panel) views of the V configuration for the intermediate electrodes (molybdenum pins). A portion of the main electrode assembly and the bottom plate for the laser head have, for clarity, been removed. Note that the upper and lower panels are not drawn to the same scale.

Most of the experimental results presented in Sec. 3 for the XeF(C→A) and iodine 1.3-μm lasers were obtained with the in-line and V configurations, respectively.

2.4 *Erosion of the Dielectric Surface*

A critical parameter determining the ultimate utility of optically pumping atomic or molecular lasers with surface discharges is the lifetime of the dielectric surface itself. For this reason, several measurements of the surface erosion rate were made with the system operating at full power (2.5 kJ stored, $V = 30$ kV). Figure 7 is a profile of the surface of a machinable glass ceramic (MACOR) dielectric, recorded with a microstylus (Dektak) after more than 500 shots of the system on the same surface. Representative of other profiles obtained during these tests, the data of Fig. 7 show the nearly symmetrical channel to have a peak depth of ≈ 50 μm and a FWHM of ≈ 0.8 cm. Thus, the average erosion rate is $\lesssim 0.1$ μm/shot. Other tests confirm the results of Fig. 7. Specifically, for a MACOR dielectric, which has a nominal composition[25] of $\approx$46% SiO_2, 16% Al_2O_3, and 17% MgO, the measured erosion rates ranged from 0.06 to 0.3 μm $shot^{-1}$, and varied by $<60\%$ along the discharge path (i.e., axially). The data suggest that the erosion rate is largest for the first few tens of shots on a new dielectric surface but quickly falls to $\lesssim 0.1$ μm $shot^{-1}$ thereafter. Preliminary tests with alumina (Al_2O_3) and SiC-coated surfaces indicate that they will exhibit erosion rates

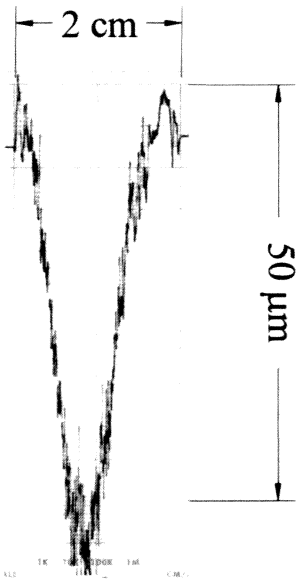

Fig. 7 Microstylus (Dektak) profile of a machinable glass ceramic dielectric surface after more than 500 shots of the laser system at full power. The FWHM of the eroded trench is ≈0.8 cm.

approximately an order of magnitude smaller than these values, which will be required for an acceptable lifetime ($>10^5$ shots for a single dielectric).

2.5 *Repetitively Pulsed Operation*

Although this system has been operated almost exclusively in the single-shot mode, it was designed and constructed so as to be capable of operation at pulse repetition frequencies (PRFs) of 1 to 5 Hz. The issues that affect repetitive operation include rapid recharging of the capacitor bank, reliable holdoff and triggering characteristics, the continuous introduction or recovery of laser fuel, clearing debris and particulates from the optical path and (as discussed earlier) electrode and dielectric surfaces, and maximizing the life of high-stress components. With respect to the former, the HV power supplies first used with this system to charge the capacitor bank were a 30-kV, 10-mA system and, subsequently, an ALE model 152 L supply, rated at 40 kV and 1.5 kJ s^{-1}. The latter supply permitted recharging of the bank in less than 10 s, but introduced electrical transients that compromised the holdoff characteristics of the power generator and triggering circuitry. More recently, replacing the earlier power supplies with an ALE model 830 L unit (40 kV, 8 kJ s^{-1}) has allowed for the capacitor bank, storing up to 4.5 kJ (for $V=40$ kV), to be charged in <1 s. It should also be mentioned that the capacitors in the bank were rated conservatively. They were designed to operate up to 100 Hz and, largely because of the small degree of current reversal to which the capacitors are subjected during each shot, have an expected survival of 90% after 10^8 shots. Furthermore, tests indicate that prefiring of the system is minimal for PRFs ≤ 5 Hz.

A longitudinal flow system was also designed that allows for replacing the gas mixture between shots. Although this subsystem has not as yet been tested, it provides for the removal of the fragments of the laser fuel molecular precursors and reconstitution of the gas mixture. For PRFs above ≈5 Hz, transverse flow of the gas mixture will be required. In this regard, the laser head was designed to accommodate an array of gas flow ports, dispersed along the length of the surface discharge on both sides of the chamber, thereby allowing for gas flow along the coordinate perpendicular to the axes of both the laser itself and the ballasting pins (cf. Fig. 4).

3 Laser Experiments

3.1 *XeF: Gain and Laser Measurements*

Although laser experiments have been carried out for both the B→X and C→A transitions of XeF in the UV and blue-green, respectively, most of the results reported here are associated with the visible band, which, because of its spectral breadth, is of interest for its potential as a high-power amplifier for femtosecond pulses.[26]

As in several previous experiments,[10,11,13,14–19,24] excitation of the XeF ($B\,^2\Sigma^+_{1/2}$) state is accomplished by the photodissociation of XeF_2 in the VUV. This is an efficient process, having a quantum yield greater than 25% for photoexcitation wavelengths between 155 and 175 nm, and a maximum value of 30% at $\lambda \approx 165$ nm.[27] The threshold photoexcitation wavelength for accessing the B state is 220 ± 2 nm,[27] and the peak absorption cross section exceeds 6×10^{-17} cm^2 (155–165 nm). Xenon difluoride vapor was introduced to the laser chamber by passing a preheated gas mixture over XeF_2 crystals. The XeF_2 number density at the laser chamber was monitored continuously by measuring the absorption of the laser gas mixture ($Ar/N_2/SF_6/XeF_2$) at 254 nm with a Hg pen lamp, a narrow-bandpass filter, and a photomultiplier. The partial pressure of the XeF_2 vapor was typically in the range of 1 to 3 Torr.[28] Argon was chosen to be the primary constituent in the gas mixture for several reasons, the foremost of which is that early studies of surface discharges found consistently that Ar provided the highest UV and VUV intensities.[6] It should also be mentioned that all pressures (except the XeF_2 vapor pressure) were measured with capacitance manometers and the results reported here were obtained with gas mixtures under static conditions.

Fluorescence and laser waveforms for the XeF(B→X) transition, representative of those observed throughout these experiments, are presented in Fig. 8. Recorded by viewing with a photomultiplier the axis of the surface discharge chamber through two 1-mm-diam. pinholes (spaced by 37.5 mm) and a neutral density filter, the fluorescence waveform in the upper panel of the figure shows both the initial fluorescence peak (intensity increases downward) following ignition of the surface discharge, and a second pulse arising from pump radiation scattered by the shock wave propagating away from the surface of the discharge. Owing to the large photoabsorption cross section of XeF_2 in the VUV, the pump bleaching wave has a measured velocity of ≈3 cm μs^{-1} (Refs. 16, 19, 29). Lasing on the B→X band was also readily obtained by installing a resonator, consisting of two spherical mirrors having transmissions of 0.2% at 351 nm, around the laser head. The oscillogram in the lower half of Fig. 8 shows the laser pulse (attenuated by a neutral density filter) to have a nominal

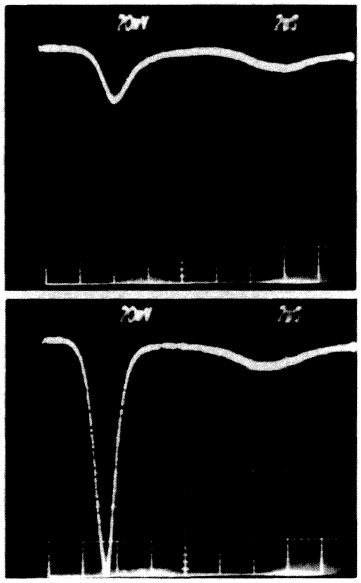

Fig. 8 XeF(B→X) fluorescence (top) and laser waveforms. For both oscillograms, intensity increases downwards, and the time base is 2 μs per large division. The gas mixture associated with the waveforms consists of 570 Torr Ar, 190 Torr N_2, 4.0 Torr SF_6, and 1.5 Torr XeF_2. To avoid saturation of the photomultiplier, the laser intensity has been attenuated with a neutral density filter.

temporal width of $\approx 1.4\ \mu$s, which is typically $\approx 20\%$ smaller than that for the fluorescence waveform. Both of the waveforms of Fig. 8 were obtained for a gas mixture of 570 Torr Ar, 190 Torr N_2, 4.0 Torr SF_6, and 1.5 Torr XeF_2. The function of SF_6 in the gas mixture is to remove, by dissociative attachment, low-energy electrons produced by photoionization of the constituents of the gas mixture. Quenching of the XeF(B, C) excited species by superelastic collisions can be a significant loss mechanism at the optical pumping rates available with high-power surface discharges ($\sim 10^{22}$ to 10^{23} photons $cm^{-2}\ s^{-1}$).[16,30]

Gain measurements on the C→A band of XeF were made with the experimental arrangement shown schematically in Fig. 9. The multiline output of an Ar ion laser was coupled into a multimode fiber and, after emerging from the fiber, collimated with a microscope objective and spatially filtered by a 1.2-mm-diam pinhole. After four passes through the active medium, the probe laser radiation im-

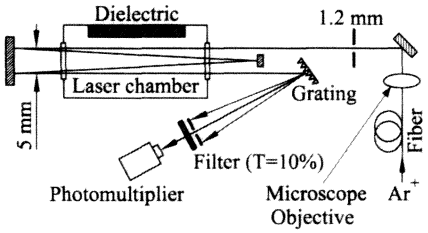

Fig. 9 Schematic diagram of the experimental arrangement for measuring gain on the C→A transition of XeF. The diffraction grating selected the 488-nm line of the Ar ion laser as the probe wavelength, and, after passing through a second pinhole and a low-pass ($\lambda \leq 650$ nm) or neutral density filter, the probe beam was detected by a photomultiplier.

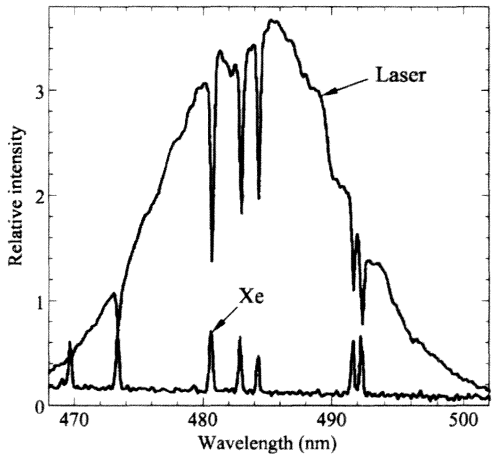

Fig. 10 XeF(C→A) laser spectrum produced by optically pumping a 570 Torr Ar, 190 Torr N_2, 4 Torr SF_6, and 1.6 Torr XeF_2 mixture with the surface discharge. The lower trace is the emission spectrum of a Xe pen lamp over the same region. All of the absorption features in the laser spectrum are assignable to 6p′, 7p ←6s$[3/2]_1$ transitions of atomic Xe.

pinged on a diffraction grating, which selected the 488-nm line for observation. Inside the laser head, the distance of the closest pass of the probe beam from the surface discharge was 1.5 cm. Although peak XeF(C→A) gain is known to occur at ~480 nm,[31] several measurements made at 488 nm for 8–10-MW cm^{-1} of power dissipated in the discharge and a gas mixture of 570 Torr Ar, 190 Torr N_2, 4.0 Torr SF_6, and 1.5–1.9 Torr XeF_2 show that the gain coefficient $\gamma \approx 0.3\%\ cm^{-1}$. At higher partial pressures of XeF_2 vapor, the gain declines sharply (to $0.12\%\ cm^{-1}$ for $p_{XeF_2} = 2.4$ Torr, for example). These values compare favorably with those measured in surface discharge devices of higher power (up to $\approx 42\ MW\ cm^{-1}$ and active lengths of 1.7 m).[15–17] Recalling that the C→A stimulated emission cross-section is $\approx 9 \times 10^{-18}\ cm^2$ (assuming a bandwidth of 60 to 70 nm FWHM),[31] the higher value given above for the gain coefficient implies a minimum population inversion of $\approx 3 \times 10^{14}\ cm^{-3}$.

When an optical cavity, consisting of a high reflector ($R > 99.9\%$ at 480 nm) with a radius of curvature of 5 m and a flat output coupler having a transmission of 1–5% at 480 nm, was installed around the active medium, lasing was observed in the blue-green. Both of the mirrors were antireflection-coated for 351 nm and had an Al_2O_3 overcoat that allowed them to be placed in direct contact with the corrosive laser gas mixture.[32] After months of laser experiments, no signs of mirror surface degradation were noticeable. The XeF(C→A) laser spectrum, recorded with a 0.25-m spectrograph (600-line mm^{-1} grating, blaze wavelength of 240 nm, 25-μm slits, operated in second order) and a diode array, is shown in Fig. 10 for a gas mixture of 570 Torr Ar, 190 Torr N_2, 4 Torr SF_6, and 1.6 Torr XeF_2. The lower trace in the figure is the emission spectrum from a Xe pen lamp over the same region. Note that the only absorption features appearing in the spectrum are attributed to transitions originating from the 6s$[3/2]_1$ ($^3P_1$ in *LS* coupling notation) excited state of atomic Xe, and terminating

Fig. 11 Photograph of the surface discharge system in operation. Most of the capacitor bank is housed behind the Al panel, but several additional capacitors, installed to attain an enhanced energy storage capacity, are mounted on the top of the system. The vacuum and gas-handling systems and power supplies are in the rack at the left.

at the $6p'[3/2]_{1,2}$ levels or the various fine structure sublevels of the $7p[3/2]_J$ state. Although other Xe transitions (originating from the $6s[3/2]_2$ metastable state), superimposed onto the C→A laser spectrum, were observed in Ref. 31, the appearance of the $Xe(6s\,^3P_1)$ state in absorption is to be expected, since it is optically connected to ground by the $6s(^3P_1)\leftarrow 5p^6(^1S_0)$ resonance transition. Owing to resonance trapping, the effective lifetime of the $^3P_1$ state will rise rapidly during the optical pumping pulse because of the increasing Xe partial pressure (and concomitant depletion of the XeF_2 laser fuel). It should also be noted that the number of absorption lines observed in the present experiments (cf. Fig. 10) is smaller than that reported by Bischel et al.,[31] who demonstrated lasing on the XeF(C→A) transition by photodissociating XeF_2 with VUV radiation ($\lambda \approx 172$ nm) from the Xe_2 excimer. The reasons for the difference are not clear, but it is interesting that it was found in Ref. 31 that substituting N_2 for Ar as the buffer gas completely eliminated absorption features from the laser spectrum. Finally, comparing Fig. 10 with XeF(C→A) laser spectra associated with electron beam or discharge pumping of the molecule[33–35] vividly illustrates one advantage of optical excitation—the elimination of virtually all atomic and molecular absorbing species that can seriously limit the laser's output power.

With 5% of cavity output coupling at 480 nm ($\leq 7\%$ for $450 \leq \lambda \leq 490$ nm), the maximum output energy obtained to date on the XeF(C→A) transition is 53 mJ in ≈ 1.5-μs FWHM pulses. Several factors, including the resonator design and clear aperture available with the present laser-head design, are limiting the single-pulse energies. With regard to the former, for example, experiments conducted with plane-plane resonators[16,17] have been successful in efficiently extracting the energy stored in the active medium. Also, since the data available in the literature for the surface-discharge-pumped C→A laser suggest that the output energy rises nonlinearly with the power dissipated per unit length of the discharge,[18] experiments with the present laser-head design but at power dissipations in the 15- to 25-MW cm^{-1} range are expected to yield single-pulse energies approaching 1 J. Another avenue to improving extraction efficiency is to operate the surface discharge system as an amplifier and seed the active volume with injected pulses from a long pulse (0.5 to 1 μs) oscillator.

As reported previously,[19] the XeF(C→A) output pulse energy is maximum for XeF_2 partial pressures of 1.4 to 1.5

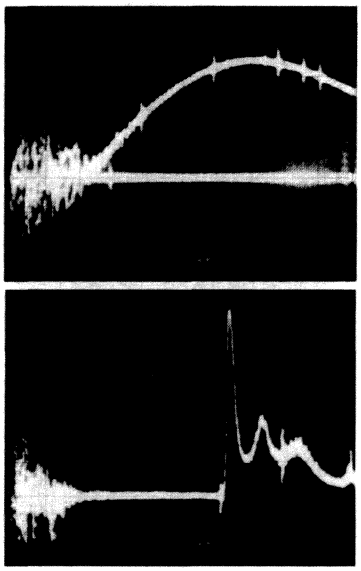

Fig. 12 Oscillograms of (top) the optical pumping pulse produced by the surface discharge, and (bottom) the iodine 1.3-μm laser waveform for a mixture of $\approx$620-Torr Ar, $\sim$190 Torr N_2, 7.5 Torr SF_6, and 18 Torr C_3F_7I. The time base for both waveforms is 1 μs/div.

Torr [$(5.0-5.3)\times10^{16}$ cm^{-3} at 300 K] and declines rapidly at higher pressures. Not surprisingly, this behavior reflects the dependence of the gain coefficient on the XeF_2 number density discussed earlier. A photograph of the surface discharge system producing a XeF(C$\rightarrow$A) laser pulse is presented as Fig. 11.

3.2 *Iodine Laser (1.315 μm) Results*

A series of laser experiments was also conducted for the 1.315-μm transition ($5p\,^2P_{1/2}\rightarrow5p\,^2P_{3/2}$) of atomic iodine. As noted earlier, Beverly and co-workers[5,7] were the first to point out the advantages of optically pumping the iodine photodissociation laser with deep UV radiation from a surface discharge and, in 1977, reported that nearly 10% of the stored electrical energy could be converted by the surface discharge into optical energy in the appropriate wavelength region (250–290 nm for C_3F_7I).

Throughout most of these experiments, C_3F_7I served as the molecular precursor, and the optimal gas mixture (with respect to single pulse laser energy) was found to be $\approx$620 Torr Ar, $\approx$190 Torr N_2, 7.5 Torr SF_6, and 18 to 20 Torr C_3F_7I. The relatively large partial pressure of the iodine-bearing molecule is understandable because of its small absorption cross section σ_a for $4\leq\hbar\omega\leq5$ eV ($\sigma_a\approx3\times10^{-19}$ cm^2 for C_3F_7I at $\lambda=270$ nm, for example), thus requiring at least 15 to 20 Torr of C_3F_7I to ensure that $(\sigma_a\cdot[C_3F_7I])^{-1}$, where square brackets denote number density, is on the order of the transverse dimensions of the optical resonator (a few centimeters). In fact, from the perspective of the optical absorption depth seen by 250- to 300-nm photons propagating away from the surface discharge, one might expect even higher C_3F_7I partial pressures to be required (25 to 30 Torr). However, collisional quenching of the $I(^2P_{1/2})$ upper laser level by C_3F_7I becomes of increasing importance as the partial pressure is raised and is responsible for the somewhat lower value of $[C_3F_7I]$ at which maximum output pulse energy is obtained. The optical cavity again comprised a high reflector at 1.3 μm, having a radius of curvature of 5 m, and a flat mirror having a transmission of 10% at the laser wavelength. Maximizing the laser output energy with respect to cavity output coupling has not yet been investigated, but estimates indicate that the optimal output coupling mirror transmission is $\approx$30%.

As reported previously,[19] the dependence of laser output energy on the C_3F_7I partial pressure displays a rather broad maximum centered at $\approx$20 Torr. Single-pulse energies exceeding 0.7 J were measured with a calibrated pyroelectric detector, and burn patterns show the beam to be highly multimode with a nearly square cross-sectional profile. The laser output pulses were monitored with an InGaAs photodiode detecting energy removed from the beam by a microscope slide. As illustrated in Fig. 12, most of the energy is extracted in a $\approx$300-ns-FWHM gain-switched spike, followed ≈1 μs later by a second, weaker pulse. Also, the onset of lasing occurs near peak emission from the surface discharge (≈4 μs following ignition of the discharge).

Several experiments were also carried out with CF_3I as the iodine donor, and, as expected, significantly lower energies but similar laser pulse waveforms were observed.

4 Summary and Conclusions

The design of a compact surface discharge laser system and its application to pumping the XeF(C$\rightarrow$A) and $I(^2P_{1/2}\rightarrow{}^2P_{3/2})$ photodissociation lasers has been described. Although having a total footprint of only 0.6 m^2, this system offers an active length of $\approx$50 cm and provides at least 8 to 10 MW of power dissipated per centimeter of discharge. Minimizing the inductance of the system resulted in a generator having an impedance that is well matched to the discharge, and the dissipation of $\approx$80% of the stored electrical energy in the surface discharge in the first half cycle of the current waveform. Detailed studies of the erosion of the surface dielectric were carried out and show, over several hundred shots, mass erosion rates of $\lesssim0.1$ μm shot^{-1} for a machinable glass ceramic surface. It is expected that the use of more robust refractory materials, such as alumina and pyrolytic boron nitride, will lower the erosion rates by another order of magnitude.

Pulse energies above 50 mJ were obtained on the C$\rightarrow$A band of XeF with 5% of cavity output coupling and a mixture of Ar, N_2, SF_6, and XeF_2 vapor. For the atomic iodine system, laser pulse energies exceeding 0.7 J were recorded with C_3F_7I as the iodine donor and 10% of cavity output coupling at 1.3 μm. Optimization of the output coupling and installing a second discharge channel will undoubtedly improve significantly the laser output energies obtainable from this system. This is expected to be particularly true for the XeF(C$\rightarrow$A) oscillator, for which the measured gain coefficient at 488 nm (0.3% cm^{-1}) is comparable to the values reported previously for much larger surface discharge laser systems dissipating as much as $\approx$40 MW per centimeter of discharge length. One concludes that the extraction of energy stored in the laser me-

dium appears to be the primary factor presently limiting the efficiency of this device. Straightforward steps to increase the extraction efficiency of this system include improving the clear aperture and resorting to a folded resonator design. Nevertheless, the detailed tests of this surface discharge system, carried out over a period of more than two years, demonstrate that a practical, high-power, and yet compact device can be realized that is attractive either as an oscillator or as a seeded amplifier.

Acknowledgments

The expert technical assistance of K. M. Collier, K. K. King, C. J. Wagner, and N. P. Ostrom is gratefully acknowledged. This work was partially supported by the Office of Naval Research and the U.S. Air Force Phillips Laboratory under contract no. N00014-93-1-0069.

References

1. See, for example, J. G. Eden, *Photochemical Vapor Deposition*, Wiley-Interscience, New York (1992).
2. For cleaning of electronic surfaces with ultraviolet radiation, see, for example, S. J. Pearton, F. Ren, C. R. Abernathy, W. S. Hobson, and H. S. Luftman, *Appl. Phys. Lett.* **58**, 1416 (1991) and references cited therein.
3. J. R. Woodworth and P. F. McKay, *J. Appl. Phys.* **58**, 3364 (1985).
4. V. S. Zuev and L. D. Mikheev, *Photochemical Lasers*, Harwood Academic Publishers, Chur, Switzerland (1991).
5. R. E. Beverly III, *J. Appl. Phys.* **46**, 3203 (1975).
6. R. E. Beverly III, R. H. Barnes, and P. K.-L. Yin, *Opt. Commun.* **14**, 412 (1975).
7. R. E. Beverly III, R. H. Barnes, C. E. Moeller, and M. C. Wong, *Appl. Opt.* **16**, 1572 (1977); R. E. Beverly III, *Appl. Phys. Lett.* **58**, 1024 (1991).
8. A. V. Belotserkovets, V. A. Gaidash, G. A. Kirillov, S. B. Kormer, V. A. Krotov, Yu. V. Kuratov, S. G. Lapin, V. M. Murugov, N. N. Rukavishnikov, V. A. Samylin, N. A. Cherkesov, and V. I. Shemyakin, *Sov. Tech. Phys. Lett.* **5**, 80 (1979).
9. See, for example, G. N. Tsikrikas, A. A. Serafetinides, and A. D. Papayannis, *Opt. Commun.* **132**, 295 (1996), and references cited therein.
10. N. G. Basov, V. S. Zuev, L. D. Mikheev, D. B. Stavrovskii, and V. I. Yalovoi, *Sov. J. Quantum Electron.* **7**, 1401 (1977) [*Kvantovaya Elektron. (Moscow)* **4**, 2453 (1977)].
11. J. G. Eden, *Opt. Lett.* **3**, 94 (1978).
12. T. E. Sharp, Th. Hofmann, C. B. Dane, W. L. Wilson, Jr., F. K. Tittel, and P. J. Wisoff, *Opt. Lett.* **15**, 1461 (1990).
13. R. W. Waynant and J. G. Eden, *IEEE J. Quantum Electron.* **QE-15**, 61 (1979); R. W. Waynant, *Appl. Phys. Lett.* **36**, 493 (1980).
14. G. N. Kashnikov, N. P. Kozlov, V. A. Platonov, V. A. Reznikov, and V. A. Sorokin, *Sov. J. Quantum Electron.* **14**, 1422 (1984) [*Kvantovaya Elektron. (Moscow)* **11**, 2129 (1984)].
15. V. S. Zuev, G. N. Kashnikov, N. P. Kozlov, S. B. Mamaev, V. K. Orlov, Yu. S. Protasov, and V. A. Sorokin, *Sov. J. Quantum Electron.* **16**, 1665 (1986) [*Kvantovaya Elektron. (Moscow)* **13**, 2521 (1986)].
16. V. S. Zuev, G. N. Kashnikov, V. V. Kirilenko, S. B. Mamaev, V. A. Sorokin, and V. F. Sukhorukov, *Sov. J. Quantum Electron.* **19**, 748 (1989) [*Kvantovaya Elektron. (Moscow)* **16**, 1154 (1989)].
17. V. S. Zuev, G. N. Kashnikov, and S. B. Mamaev, *Sov. J. Quantum Electron.* **22**, 973 (1992) [*Kvantovaya Elektron. (Moscow)* **19**, 1047 (1992)].
18. B. A. Knecht, R. D. Fraser, D. J. Wheeler, C. J. Zietkiewicz, L. D. Mikheev, V. S. Zuev, and J. G. Eden, *Proc. SPIE* **2118**, 59 (1994).
19. B. A. Knecht, R. D. Fraser, D. J. Wheeler, C. J. Zietkiewicz, L. D. Mikheev, V. S. Zuev, and J. G. Eden, *Opt. Lett.* **20**, 1011 (1995).
20. R. W. F. Gross, L. E. Schneider, and S. T. Amimoto, *Appl. Phys. Lett.* **53**, 2365 (1988).
21. M. L. Sentis, Ph. Granier, F. Chazaud, W. I. Marine, M. Gerry, and R. C. Sze, *Appl. Surf. Sci.* **69**, 185 (1993).
22. F. Chazaud, M. L. Sentis, H. C. Le, H. Rigneault, Ph. C. Delaporte, and W. I. Marine, *Appl. Phys. Lett.* **65**, 1626 (1994).
23. V. I. Tcheremiskin, M. L. Sentis, Ph. C. Delaporte, V. S. Zuev, and L. D. Mikheev, *J. Appl. Phys.* **80**, 2094 (1996).
24. M. L. Sentis, V. I. Tcheremiskine, Ph. C. Delaporte, L. D. Mikheev, and V. S. Zuev, *Appl. Phys. Lett.* **70**, 1198 (1997).
25. Corning Glass Works, Corning Technical Bulletin No. 1-R79.
26. V. I. Tcheremiskine, M. L. Sentis, and L. D. Mikheev, *Appl. Phys. Lett.* **81**, 403 (2002).
27. N. K. Bibinov, I. P. Vinogradov, L. D. Mikheev, and D. B. Stavrovskii, *Sov. J. Quantum Electron.* **11**, 1178 (1981) [*Kvantovaya Elektron. (Moscow)* **8**, 1945 (1981)].
28. F. Schreiner, G. N. McDonald, and C. L. Chernick, *J. Phys. Chem.* **72**, 1162 (1968).
29. V. S. Zuev, L. D. Mikheev, and D. B. Stavrovskii, *Sov. J. Quantum Electron.* **14**, 1174 (1984) [*Kvantovaya Elektron. (Moscow)* **11**, 1750 (1984)].
30. J. G. Eden and S. K. Searles, *Appl. Phys. Lett.* **29**, 356 (1976).
31. W. J. Bischel, D. J. Eckstrom, H. C. Walker, Jr., and R. A. Tilton, *J. Appl. Phys.* **52**, 4429 (1981).
32. V. D. Vvedenskii, L. D. Mikheev, S. I. Sagitov, V. F. Sukhoverkhov, and D. B. Stavrovskii, *Inorg. Mater. (Transl. of Neorg. Mater.)* **23**, 1504 (1987).
33. C. H. Fisher, R. E. Center, G. J. Mullaney, and J. P. McDaniel, *Appl. Phys. Lett.* **35**, 26 (1979).
34. R. Burnham, *Appl. Phys. Lett.* **35**, 48 (1979).
35. W. E. Ernst and F. K. Tittel, *Appl. Phys. Lett.* **35**, 36 (1979).

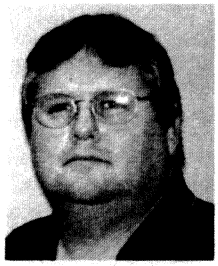

Brent A. Knecht earned his Master of Science degree in electrical engineering in 1995 from the University of Illinois at Urbana-Champaign under the direction of Professor J. G. Eden. His graduate work involved the electrical, mechanical, and optical design of a novel VUV optical pump, and using that apparatus to construct and characterize gas lasers and optical amplifiers. Since then, Knecht has worked as a product design engineer for midwest manufacturing firms. His industry experience includes software and electronic hardware development of mid-volume products for industrial and test equipment markets. He is currently employed by Griffin Analytical Technologies, Inc., in the design of electronics for a field-portable miniature ion-trap mass spectrometer.

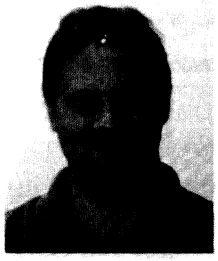

Richard D. Fraser received his PhD degree in electrical engineering from the University of Illinois at Urbana-Champaign in 1994. Following several years of designing and developing laser medical and micromachining systems with Cynosure and Resonetics, he cofounded Realized Technologies, Inc. Dr. Fraser is currently the vice president of the firm and leads development teams for new medical products.

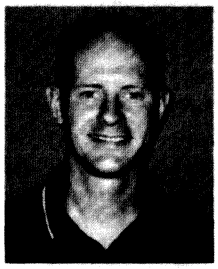

David J. Wheeler received his BS degree in 1994 and his MS degree in 1998 in electrical and computer engineering from the University of Illinois, Urbana-Champaign. He specialized in quantum electronics. He has been employed for the past five years as a network engineer at the National Center for Supercomputing Applications (NCSA) at the University of Illinois. He works to maintain and advance networks at NCSA, designing and deploying microwave point-to-point wide-area networks and wireless local-area networks. He is also engaged in the design and deployment of optical networks, including DWDM network equipment in support of the NSF-funded TeraGrid project.

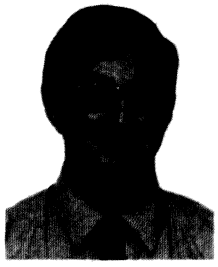

Chris J. Zietkiewicz received his BS, MS, and PhD degrees from the University of Illinois in electrical engineering. He joined Melles Griot in 1995 as a staff engineer designing various gas, diode, and DPSS laser support electronics. He is currently employed as site manager at Melles Griot Electro-Optics in Longmont, Colorado.

Andrey A. Senin received his degree of Radio Engineer (with high honors) from the Bauman Moscow State Technical University (BMSTU) in 1992, and his MS degree in electrical engineering from the University of Illinois at Urbana-Champaign (UIUC) in 1999. He expects to receive the PhD degree from UIUC in 2003. At BMSTU, he conducted research in the field of spread-spectrum communications. Since joining the Laboratory for Optical Physics and Engineering at UIUC, he has pursued interdisciplinary research, including the application of digital signal processing to ultrafast laser spectroscopy, and upconversion fiber lasers and amplifiers. He has published over twenty journal and conference papers. Senin is a student member of the Lasers & Electro-Optics (LEOS) and Communications (ComSoc) Societies of the IEEE, and SPIE.

L. D. Mikheev received his MS degree in radiophysics (1966) from the Moscow Physical-Technical Institute, and his PhD degree in quantum radiophysics (1974) from the P. N. Lebedev Physical Institute of the Russian Academy of Sciences. He joined the P. N. Lebedev Physical Institute in 1966, and since 1990 has held the position of head of the Photochemical Processes Laboratory. His research group pioneered the research and development of optically pumped photochemical lasers based on electronic molecular transitions and has demonstrated laser action on numerous transitions in the spectral range from the near IR to the UV by excitation with broadband radiation from open discharges and strong shock waves. His current research interests focus on the direct amplification of femtosecond optical pulses in photochemically driven broadband active media, with emphasis on the optically pumped XeF(C-A) transition. Dr. Mikheev is a member of the Optical Society of America. He has published more than one hundred papers and is the coauthor of two books.

Vitaly S. Zuev is a graduate of the Moscow Institute of Physics and Technology (1957). Since March 1957, he has been with the P. N. Lebedev Physical Institute of the Russian Academy of Sciences, where he now holds the title of professor. He was awarded a Candidate of Science degree in physics and mathematics for his study of the ND_3 maser in 1963, a Doctor of Science degree in physics and mathematics for his study of the photodissociation laser pumped by shock and thermal waves in 1970, and his professorship in radiophysics in 1981, all three from the Lebedev Institute. Now he occupies himself with solving the problem of subwavelength focusing of laser beams. He has worked for some time at the University of Illinois in Urbana-Champaign with Prof. J. G. Eden studying the problem of gas laser pumping with radiation produced by high-current open discharges, and the physics of atom-atom photoassociation in gases and vapors.

J. Gary Eden received his BS degree in electrical engineering (high honors) from the University of Maryland, College Park, MD, in 1972, and his MS and PhD degrees from the University of Illinois at Urbana-Champaign, in 1973 and 1976, respectively. In 1975, he was awarded a National Research Council Postdoctoral Research Associateship at the U.S. Naval Research Laboratory (NRL). In November of 1976, he joined the staff of the Laser Physics Branch (Optical Sciences Division) of NRL. During his tenure at NRL, he made several contributions to the area of visible and ultraviolet lasers and gas laser spectroscopy, including the codiscovery of the KrCl laser at 222 nm and the first long-pulse (>1 μs) excimer laser. He received a Research Publication Award (1979) for his work at NRL in which he codiscovered the proton-beam-pumped laser. Since joining the faculty of the University of Illinois in 1979, he has been engaged in research in molecular and atomic laser spectroscopy, the discovery and development of ultraviolet and visible lasers, and ultrafast laser probing of wave packets and chemical dynamics. Recent accomplishments of his research group include the observation of molecular dissociation with atomic wave packets, and the development of microdischarge-based photonic devices. At the University of Illinois, he has served as assistant dean in the College of Engineering and associate dean of the Graduate College, and is currently associate vice-chancellor for research, professor in the Department of Electrical and Computer Engineering, and director of the Laboratory for Optical Physics and Engineering. He has over 180 publications and holds 18 patents. Dr. Eden is a Fellow of the IEEE, the Optical Society of America, and the American Physical Society. From 1996 through 1999, he was the James F. Towey University Scholar at the University of Illinois. He has served as editor-in-chief of the *IEEE Journal of Quantum Electronics* (1996–2002) and in 1998 was president of the IEEE Lasers and Electro-Optics Society (LEOS). Previously, he served as a member of the LEOS Board of Governors and the vice president for technical affairs. Dr. Eden received the LEOS Distinguished Service Award in 1996, and the IEEE Third Millennium medal in 2000. He was recently appointed a LEOS Distinguished Lecturer for 2003–2004.